

Regional Model Nesting within GFS Daily Forecasts Over West Africa

Leonard M. Druyan*, Matthew Fulakeza, Patrick Lonergan and Ruben Worrell

Center for Climate Systems Research, Columbia University and NASA/Goddard Institute for Space Studies, Armstrong Hall, 2880 Broadway, New York, NY 10025, USA

Abstract: The study uses the RM3, the regional climate model at the Center for Climate Systems Research of Columbia University and the NASA/Goddard Institute for Space Studies (CCSR/GISS). The paper evaluates 30 48-hour RM3 weather forecasts over West Africa during September 2006 made on a 0.5° grid nested within 1° Global Forecast System (GFS) global forecasts. September 2006 was the Special Observing Period #3 of the African Monsoon Multidisciplinary Analysis (AMMA). Archived GFS initial conditions and lateral boundary conditions for the simulations from the US National Weather Service, National Oceanographic and Atmospheric Administration were interpolated four times daily. Results for precipitation forecasts are validated against Tropical Rainfall Measurement Mission (TRMM) satellite estimates and data from the Famine Early Warning System (FEWS), which includes rain gauge measurements, and forecasts of circulation are compared to reanalysis 2. Performance statistics for the precipitation forecasts include bias, root-mean-square errors and spatial correlation coefficients. The nested regional model forecasts are compared to GFS forecasts to gauge whether nesting provides additional realistic information. They are also compared to RM3 simulations driven by reanalysis 2, representing “high potential skill” forecasts, to gauge the sensitivity of results to lateral boundary conditions. Nested RM3/GFS forecasts generate excessive moisture advection toward West Africa, which in turn causes prodigious amounts of model precipitation. This problem is corrected by empirical adjustments in the preparation of lateral boundary conditions and initial conditions. The resulting modified simulations improve on the GFS precipitation forecasts, achieving time-space correlations with TRMM of 0.77 on the first day and 0.63 on the second day. One real-time RM3/GFS precipitation forecast made at and posted by the African Centre of Meteorological Application for Development (ACMAD) in Niamey, Niger is shown.

1. INTRODUCTION

The African Monsoon Multidisciplinary Analysis (AMMA) aims to improve our understanding of the climate of West Africa, especially the variability of precipitation systems (Redelsperger *et al.* [1]). During the AMMA special observing periods, June-September 2006, Météo-France provided daily numerical weather forecasts based on ARPEGE (Action de Recherche Petite Echelle Grande Echelle) global models and the ALADIN (Aire Limitée Adaptation Dynamique Développement International) limited area model. Nuret *et al.* [2] evaluate the performance of those ARPEGE and ALADIN daily weather forecasts over West Africa. They found that “the skill of Météo France models in predicting precipitation is low...” and that the high horizontal resolution of ALADIN (10 km grid) increases the positive bias of simulated precipitation compared to the two ARPEGE global models, both with grid spacing of 50 km over West Africa. Over the four-month period, ALADIN precipitation rates over the whole domain were 42% higher than observations. Regionally, the bias was especially high over the Fouta-Djallon mountains along the southwest coast of Guinea and within the main rain band between 10°W - 5°E . The European Centre for Medium Range Weather Forecasts (ECMWF) operational precipitation forecasts for the same period showed less bias over this

central region (Nuret *et al.* [2]). Druyan *et al.* [3] also found positive bias in seasonal simulations of precipitation with the model used here and three other regional models. Reed *et al.* [4] evaluated the structure and characteristics of African easterly wave disturbances in earlier ECMWF operational analyses and forecasts, but not simulated precipitation.

RM3 is the regional climate model at the Center for Climate Systems Research of Columbia University and the NASA/Goddard Institute for Space Studies (CCSR/GISS). The RM3 driven by reanalysis data has been used to study the variability of the West African summer monsoon (Druyan *et al.* [5, 6]). Druyan *et al.* [7] show that RM3 simulations driven by NCEP reanalysis 2 (NCP2) capture the major features of a developing tropical cyclone moving from West Africa to the eastern Atlantic. The congruity of simulated daily precipitation patterns and circulation with observational evidence motivates the current evaluation of RM3 skill in daily weather forecasts.

This study analyzes 30 RM3 two-day simulations driven by NOAA Global Forecast System (GFS) global numerical forecasts and compares them to precipitation observations and simulations using alternative strategies for the RM3 initial conditions and lateral boundary conditions (LBC), described below in Section 2. The RM3/GFS system is also running at the African Centre of Meteorological Application for Development (ACMAD) in Niamey, Niger, and producing daily forecasts. See <http://www.acmad.org/en/prevision/modeles2.htm>

*Address correspondence to this author at the Center for Climate Systems Research, Columbia University and NASA/Goddard Institute for Space Studies, Armstrong Hall, 2880 Broadway, New York, NY 10025 USA; Tel: 212 678-5564; Fax: 212 678-5552; E-mail: LDruyan@giss.nasa.gov

CCSR/GISS and ACMAD are cooperating to improve RM3 performance.

2. DATA SETS, SIMULATION STRATEGIES AND MODEL DESCRIPTION

2.1. Domain and Lateral Boundary Conditions (LBC)

The RM3 computational grid uses 0.5° latitude/longitude spacing on a domain bounded by 20°S - 35°N , 35°W - 35°E and integrations are made at 28 vertical levels. The horizontal domain is the same that is used in regional model experiments for the West African Monsoon Modeling and Evaluation initiative (WAMME) (Xue *et al.* [8]; Druyan *et al.* [3]). Druyan *et al.* [3] suggest that the proximity of the western domain boundary to the African coast causes serious interference in MM5 simulations. On the other hand, ALADIN was run operationally over a domain bounded on the west by 25°W with no detectable adverse boundary effects (Nuret *et al.* [2]). LBC for driving a regional model are taken from global analyses or forecasts, usually at lower horizontal resolution than the regional model grid. In these experiments LBC were taken from each driving data set four times daily, interpolated in time and space along the RM3 domain boundaries and merged with simulated variables by weighting them with decreasing weights inward within a 3° buffer zone. In most strategies, regional models produce a higher resolution version of the driving data, called dynamic downscaling. The downscaled product is not an interpolation of the driving data. Rather, integration of the regional model produces a new analysis or forecast that presumably benefits from the regional model physics, higher resolution of specified land surface characteristics and integration of the dynamic equations on the finer grid, which allows steeper gradients.

GFS global forecasts (GFS FCST) available in real-time on a 1° grid are used here as LBC to drive the RM3 over West Africa, producing weather forecasts on the regional model 0.5° grid. The GFS forecasts are generated by a global model run at spectral resolution of T382, or the equivalent grid spacing of 40 km, with 64 vertical layers (Campana *et al.* [9]). The Global Climate and Weather Modeling Branch (GCWMB [10]) describes other features of the GFS model. Since GFS results are also available at 0.5° horizontal spacing, the research focuses more on evaluating nested RM3 performance and comparing it to GFS results than on downscaling. Note that the RM3 (but not the GFS system) was specifically optimized for simulating the West African monsoon. The present study evaluates RM3 daily forecasts, focusing on September 2006, the Special Observing Period #3 of AMMA. By considering a historical period rather than a study based on real-time data, control simulations with reanalysis are also possible. In addition to LBC from GFS real-time forecast fields, parallel experiments are made using LBC from the National Center for Environmental Prediction (NCEP) reanalysis 2 (NCPR2) (Kanamitsu *et al.* [11]), gridded at 2.5° and GFS 00 hour “forecasts” (ZHF) (gridded at 1°). NOAA uses ZHF data sets as initial conditions for the real-time GFS forecasts. Downscaled NCPR2 data sets cannot be created in real-time, but they probably demonstrate the highest potential skill of RM3 forecasts on any given day, since reanalysis should usually be a better representation of actual conditions than GFS analyses or

forecasts. An RM3 simulation using LBC from ZHF were used to create initial conditions for the forecasts, as described in the following section.

2.2. Observational Data

Precipitation simulations are validated against the Tropical Rainfall Measurement Mission (TRMM) and the Climate Prediction Center Famine Early Warning System version 2 data sets for Africa (FEWS). TRMM 3B42 V6 data are estimates of daily precipitation accumulations (Huffman *et al.* [12]) for squares of 0.5° . The daily estimates are based on a modification of the Global Precipitation Index (GPI) from GOES geostationary satellite infrared (IR) measurements. To form the final data set, GPI values are calibrated by TRMM microwave, radar, visible and IR and rain gauge observations. Ruane and Roads [13] explain the calibration of radiances to create the 3B42 data and compare TRMM precipitation climatology to other data sets. Druyan *et al.* [5] compared time series of TRMM daily estimates with 34 corresponding co-located rain gauges within a $2^{\circ} \times 2^{\circ}$ area over West Africa during July-September 2000. They found a time correlation of 0.79 in the daily precipitation variability and a correlation of 0.86 between TRMM and the RM3 simulation. Good agreement between RM3 simulated precipitation and TRMM was interpreted as evidence of mutual validation, since these are totally independent systems representing the same precipitation events.

FEWS data are based on combining rain gauge and METEOSAT remote radiometric measurements. Herman *et al.* [14] explained the methodology, but version 2 was only implemented in 2000. Druyan *et al.* [6] compare TRMM to FEWS June-September 2001-2003 means over West Africa and find TRMM values to be higher over coastal mountain ranges.

2.3. Initial Conditions for 48-Hour Forecasts

The current study focuses on 48-hour simulations, each initialized at 00 UT. Druyan and Fulakeza [15] showed that the RM3 driven by NCPR1 reanalysis data is capable of simulating precipitation rates that are highly correlated in time and location with corresponding TRMM estimates, but only after a spin-up of at least five days. This suggests that the initial conditions for RM3 forecasts may also require a spin-up to allow the RM3 to adjust to the initial meteorological data. This presents a problem since weather forecast skill decreases with elapsed time from the initial conditions. In order to overcome this challenge, initial conditions for each experimental RM3/GFS forecast described in the study are produced from a continuous RM3 simulation, begun on August 20, 2006, and driven by four times daily ZHF (hereafter RM3/GFS ZHF). Since ZHF are available from NOAA in real-time, RM3/GFS ZHF can be updated operationally up to the time of the appropriate initial conditions. Using RM3/GFS ZHF as the initial conditions for forecasts assumes that it provides a reasonably accurate analysis of atmospheric conditions that are compatible with the RM3. Druyan *et al.* [5] found that the correlation between RM3 simulations driven by NCPR1 versus observational evidence does not deteriorate with elapsed time throughout entire four-month seasons, implying that the quality of RM3/GFS ZHF for initial conditions fields can be similarly maintained. The benefit of the spin-up of initial

conditions can be appreciated by noting that parallel forecasts initialized with ZHF directly from the GFS archive are indeed inferior. In addition, 30 first day forecasts reinitialized each day with NCPR2 and driven with NCPR2 LBC are also much inferior to the continuous 30-day simulation started with a spin-up from August 15. "Inferior" in this context means exhibiting less realistic precipitation features.

In order to initialize and drive RM3 simulations with GFS data, experimentation shows that modifications need to be made in the processing of the GFS data. Without such modifications, simulations initialized and driven with GFS data sets produce prodigious amounts of rainfall, while the same model initialized and forced by reanalysis data produces a much smaller positive precipitation bias. In fact, GFS precipitation forecasts for West Africa produced by the global model are also much too rainy (Table 1). The excess simulated RM3/GFS rainfall problem is eliminated when the initial and lateral boundary conditions are prepared with an empirical adjustment that lowers temperatures used to compute initial surface pressures. In this adjustment the virtual temperature is reset to equal the temperature, as if the air were dry. The largest adjustments are therefore within the most humid locations, such as the ITCZ and the West African rain band. The lowered temperatures, in turn, increase pressure increments for extrapolation to the surface pressure from reanalysis 1000 mb or 925 mb geopotential heights. Since the largest adjustments occur in the most humid locations, they raise central pressures south of the monsoon trough more than elsewhere, effectively weakening the pressure gradients that drive the monsoon circulation. Fig. (1a) shows the differences in sea-level pressure between the September 1, 2006 simulation with modified initial and boundary conditions minus the original nested simulation. Increases in SLP of almost 1 mb near 15°N in juxtaposition with no changes over the Atlantic near 3°N indicate a reduced pressure gradient, which is consistent with weaker moisture advection and lower precipitation rates. Fig. (1b) shows the mean 925 mb moisture advection (QV9) for September 1-30 first day simulations with the modifications and Fig. (1c) without them. The modifications reduce the maximum QV9 over West Africa by 33%. The subsequent decreases of moisture convergence over West Africa are

sufficient to reduce simulated rainfall rates by at least 100% over most of the rain band. Additional more modest reductions in precipitation rate are also achieved by increasing dry entrainment as part of the moist convection calculations. This and the changes in the preparation of initial conditions and LBC are hereafter referred to as the "modifications." Note in Fig. (1) that internal feedbacks and adjustments during the 24 hour simulations eventually change QV9 over the Atlantic as well.

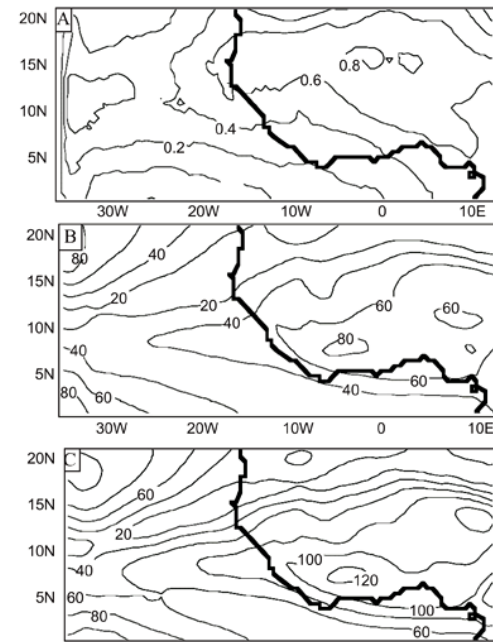


Fig. (1). Impacts of empirical adjustments of GFS initial conditions and LBC on sea-level pressure (SLP) and moisture advection: **a)** RM3/GFS FCST SLP with modified initial conditions and LBC minus RM3/GFS FCST SLP unmodified (mb) for September 1, 2006; **b)** mean 925 mb moisture advection for 30 one-day RM3/GFS FCST with modified initial conditions ($\text{g kg}^{-1}(\text{m s}^{-1})$); **c)** mean 925 mb moisture advection for 30 one-day RM3/GFS FCST unmodified ($\text{g kg}^{-1}(\text{m s}^{-1})$).

3. RESULTS

3.1. Summaries for September 2006

Fig. (2) shows the total September 2006 precipitation accumulations based on TRMM, GFS one-day forecasts and the RM3. Table 1 presents the statistics of validation of those precipitation simulations versus TRMM.

Fig. (2a) shows the total accumulated rainfall for September 2006 from TRMM estimates. The Atlantic ITCZ along 6-8°N features accumulations ranging between 200-500 mm, similar accumulations along the southwest African coast and a large orographic maximum ranging between 500-900 mm over the Cameroon Highlands. Accumulations over most of West Africa are less than 350 mm and eastern Guinea is particularly dry, receiving less than 200 mm. FEWS precipitation data for September 2006 (Fig. 2b) shows the same features with but minor inconsistencies.

Fig. (2c) shows the total precipitation accumulations for 30 one day GFS forecasts during September 2006 (hereafter

Table 1. Validation Statistics of Simulated September 2006 Accumulated Precipitation for the Area 5-12°N, 20°W-10°E Against TRMM Estimates. RM3/GFS Forecasts Represent the Sum of 30 One-Day Simulations, while RM3/NCPR2 Represents the Accumulations of Continuous 30-Day Simulations

	Bias	rms Error	Correlation Coefficient
GFS forecasts	+151 mm	218 mm	0.32
RM3/NCPR2	+101 mm	138 mm	0.63
RM3/NCPR2 modified LBC	-73 mm	97 mm	0.84
RM3/GFS forecasts first day	+3 mm	93 mm	0.60
RM3/GFS forecasts second day	-10 mm	101 mm	0.55

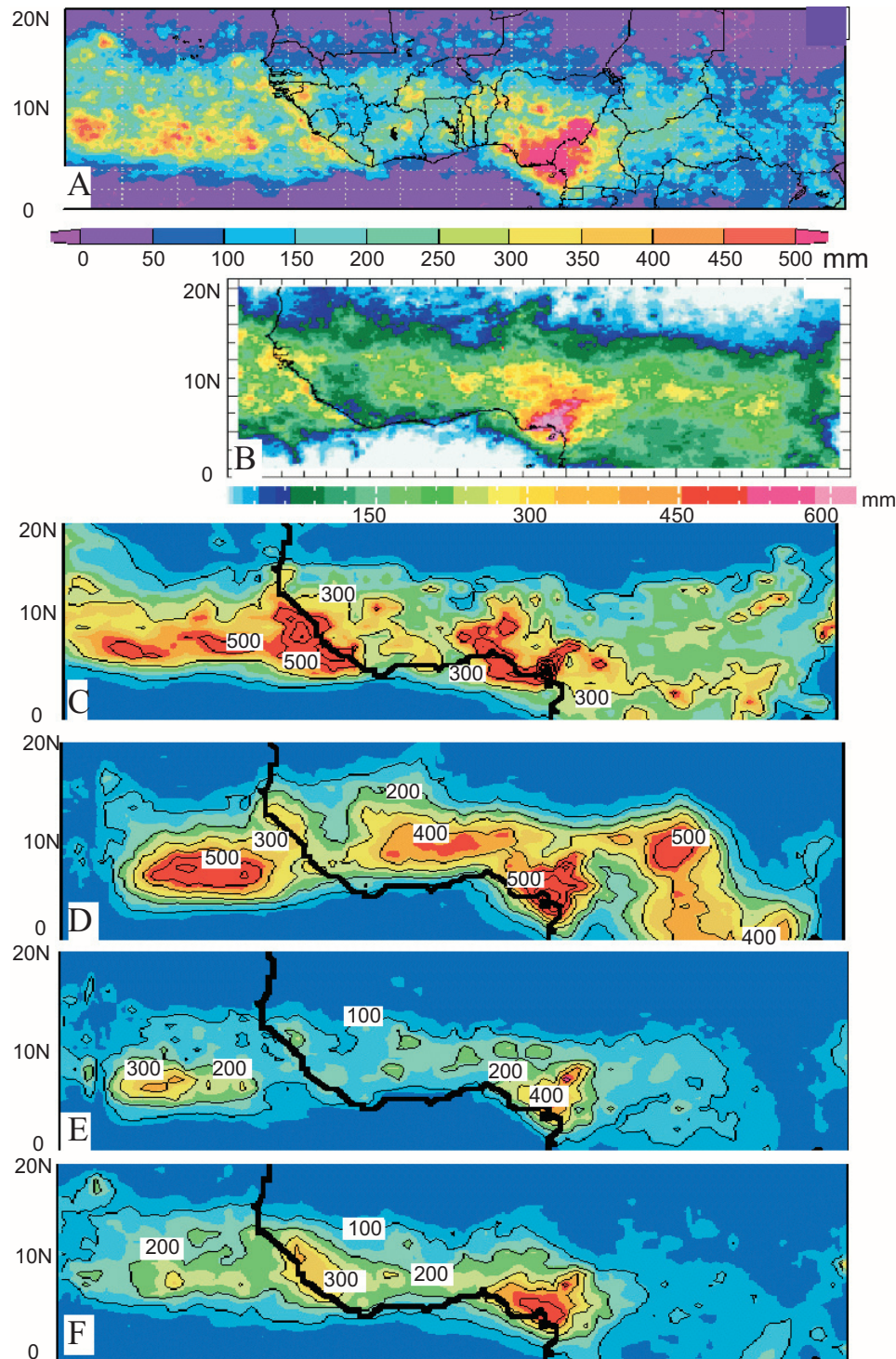


Fig. (2). Precipitation accumulations (mm) for September 2006. **a)** TRMM, **b)** FEWS, **c)** GFS one- day forecasts, **d)** RM3/NCPR2, **e)** RM3/NCPR2 with modified LBC, **f)** RM3/GFS FCST with modified LBC. TRMM data courtesy NASA's Goddard Earth Sciences (GES) Data and Information Services Center (DISC). FEWS data courtesy IRI/LDEO Columbia University.

GFS FCST), each initialized at 00 UT. The GFS coastal maximums are about 50% too high, while East Guinea and Nigeria are also too rainy. Elsewhere over West Africa, GFS FCST accumulations exceeding 300 mm cover too much area. GFS forecast precipitation was interpolated to the 0.5° grid for explicit comparison with TRMM and RM3 data. Table 1 shows that the GFS FCST bias relative to TRMM

over the validation area (hereafter Area 1: 5–12°N, 20°W–10°E) is 151 mm, which is 65% of the TRMM area mean. The root-mean-square (rms) error with respect to TRMM is 218 mm, or 94% of the TRMM area mean. The spatial correlation coefficient of GFS FCST versus TRMM over Area 1 is only 0.32.

Regional model simulation results, such as in Fig. (2d-f), show an abrupt cut-off of the Atlantic ITCZ near the western boundary, which is an adverse edge effect of the limited area domain. RM3/NCPR2 (Fig. 2d) creates an ITCZ maximum in the correct location, but with too large an area of accumulations exceeding 500 mm. The RM3/NCPR2 coastal maximum, the dry slot in the lee of the Guinea Highlands and the maximum over the Cameroon Highlands are improvements over GFS FCST perhaps attributable to the benefits of the RM3 on the 0.5° grid. However, RM3/NCPR2 exaggerates rainfall along 8°N over West Africa, and the maximum along 20°E is not validated by TRMM or FEWS observations. The bias of RM3/NCPR2 relative to TRMM over Area 1 is 101 mm (Table 1), the rms error is 138 mm and the spatial correlation coefficient is 0.63.

The continuous simulation forced by NCPR2 LBC can be improved by the modification of the LBC, as discussed above. Fig. (2e) shows a considerable reduction in the September accumulations relative to the parallel simulation with the unmodified LBC. Table 1 indicates that this simulation has a negative bias relative to TRMM over Area 1, a smaller rms error and a much improved spatial correlation coefficient of 0.84. Much of the improvement is in the reduction of precipitation accumulations over West Africa and over 20°E . Reinitializing with NCPR2 each day causes additional, unrealistic reductions in simulated precipitation (not shown).

RM3 simulations forced by unmodified GFS FCST LBC are excessively rainy and are not considered here. Fig. (2f) represents the accumulations of 30 first day simulations of RM3 forced by GFS forecasts (hereafter RM3/GFS FCST), initialized using the modification of the RM3/ZHF spin-up file, and using modified LBC. Maxima within the Atlantic ITCZ range between 200-300 mm, missing the highest TRMM observed peaks. Simulated precipitation along the Guinea coast is reasonable as are maxima within the West African rain belt. In these respects the nested RM3 forecasts improve on the original GFS FCST (Fig. 2c). Note that these RM3 simulations also do not predict heavy rainfall along 20°E . The corresponding bias of the 30 one-day simulations relative to TRMM is close to zero (Table 1), but the spatial correlation of 0.60 is much lower than for NCPR2 forced with modified LBC, probably owing to large forecast errors in the forcing data from the GFS system. Accumulations based on forecasts for the second day have only slightly poorer validation scores than for the first day. Between first day and second day forecasts for September 1-30, the Area 1 bias relative to TRMM changes from +3 mm to -10 mm, the rms error increases from 93 mm to 101 mm and the spatial correlation decreases from 0.60 to 0.55.

Hovmöller distributions show both temporal and spatial variability of simulation products. Fig. (3) compares Hovmöller time-longitude distributions of daily precipitation accumulations during September 1-30, 2006 for TRMM (Fig. 3a), GFS FCST (Fig. 3b), RM3/NCPR2 (Fig. 3c), RM3/NCPR2 with modified LBC (Fig. 3d) and RM3/GFS FCST first day and second day with modified LBC (Fig. 3e and 3f, respectively). All data are averaged over $5\text{-}15^\circ\text{N}$ and are plotted for each longitude at 0.5° intervals, $30^\circ\text{W}\text{-}10^\circ\text{E}$, except for Fig. (3b), which shows

GFS forecast data at 1° intervals. The diagonal swaths of heavy precipitation on time-longitude Hovmöller distributions indicate westward propagating systems, probably associated with AEWs (Druyan *et al.* [3]; Schmidlin *et al.* [16]). The GFS forecasts capture some of the TRMM detected swaths, but there are many discrepancies. Table 2 gives the means of the fields shown in Fig. (3) and the time-space correlations between model data and TRMM. The correlation between the data in Fig. (3b) and TRMM arranged on a 1° grid is 0.37 and the mean for GFS FCST is about 46% higher than TRMM. Fig. (3e) is based on the RM3/NCPR2 simulation. Many of the TRMM swaths are recreated, for example, the event of September 10-13, associated with the AEW that developed into Hurricane Helene (Druyan *et al.* [3]). RM3/NCPR2 underestimates maxima associated with other AEWs, and generates light rainfall between storms where TRMM indicates near zero accumulations, increasing the mean relative to TRMM by about 30%. This positive bias is caused in large measure by the inability of the RM3 to shut down precipitation completely between events, sometimes called “perpetual drizzle.” These RM3/NCPR2 results have a 0.60 correlation with TRMM, lower than correlations previously obtained when comparing June-September RM3/NCPR1 simulations to TRMM (Druyan *et al.* [6]). However, the increase of the correlation from 0.37 to 0.60 and the lower bias imply that the regional model adds additional realistic spatial and temporal detail to the simulated precipitation field. Moreover, in this experiment the RM3 is forced by a reasonable representation of actual meteorology, no doubt contributing to the skill in simulating the propagation of major precipitation bearing systems. Modifying NCPR2 LBC as explained above, additionally decreases simulated rainfall (Fig. 3d), creating more distinct breaks between systems, but lowering maxima considerably. The mean for these results is 35% lower than TRMM (Table 1), but the time-space correlation is 0.85. Results from the nested RM3/GFS FCST for the first day on the Hovmöller charts are only 14% lower than TRMM and the time-space correlation with TRMM is 0.77. For the second day the mean is 20% lower than TRMM and the correlation decreases to 0.63.

Fig. (4) shows the probability density distributions for the data presented in each of the panels of Fig. (3). The curve for GFS FCST indicates consistently higher precipitation rates than TRMM at all parts of the distribution. For example, while 20% of TRMM values $>12 \text{ mm day}^{-1}$, about 35% of GFS FCST values exceed that threshold. RM3 forced by unmodified NCPR2 LBC have a similar distribution for the lower 50%, with a better match with TRMM for the highest 10%. RM3/NCPR2 with modified LBC produce lower precipitation rates than TRMM for all but the lowest 10% of the data. The lower 50% of RM3/GFS FCST first day precipitation rates are distributed very similar to TRMM estimates, and the highest 30% favor lower values than TRMM. The top 10% of the RM3/GFS FCST for the second day shows an even wider negative departure from TRMM.

3.2. Case Study: September 10, 2006

The African easterly wave disturbance that crossed the African Atlantic coast on September 11-12, 2006 developed

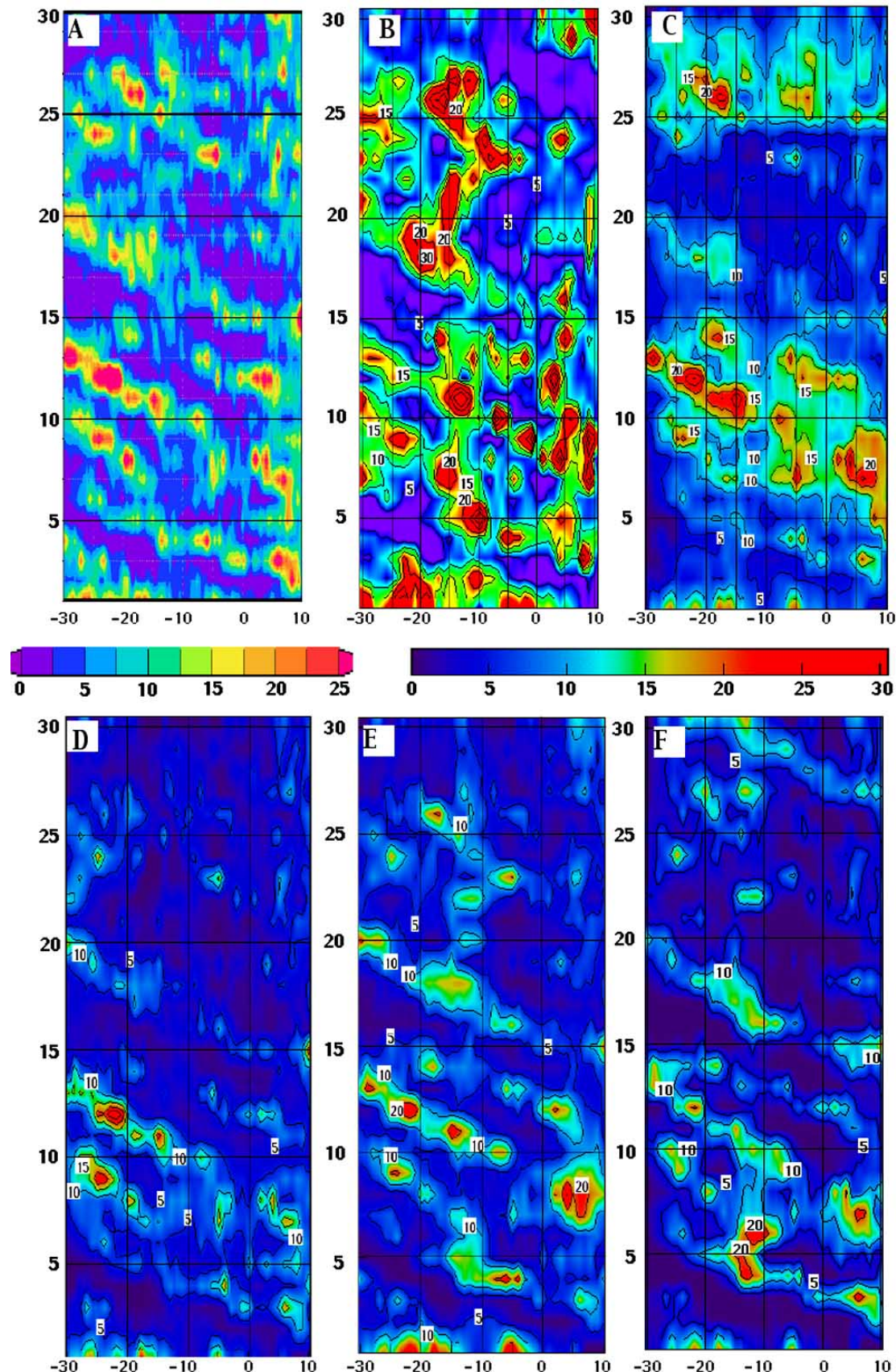


Fig. (3). Hovmöller time-longitude plots of daily precipitation accumulations (mm), averaged over 5-15°N. **a)** TRMM, **b)** GFS Fcst, **c)** RM3/NCPR2, **d)** RM3/NCPR2 with modified LBC, **e)** RM3/GFS FCST, first day, **f)** RM3/GFS FCST, second day.

Table 2. Statistics of Precipitation Data from Fig. (3). The 15°N Average Daily Precipitation is Considered at Each 0.5° (or 1° for GFS) of Longitude, 30°W-10°E. Correlation Coefficients are Between Each Time-Latitude Array and Corresponding TRMM Values

	Mean	Correlation Coefficient
TRMM	7.1 mm	1.00
GFS forecasts	10.4 mm	0.37
RM3/NCPR2	9.2 mm	0.60
RM3/NCPR2 w/modified LBC	4.6 mm	0.85
RM3/GFS forecasts first day	6.1 mm	0.77
RM3/GFS forecasts second day	5.7 mm	0.63

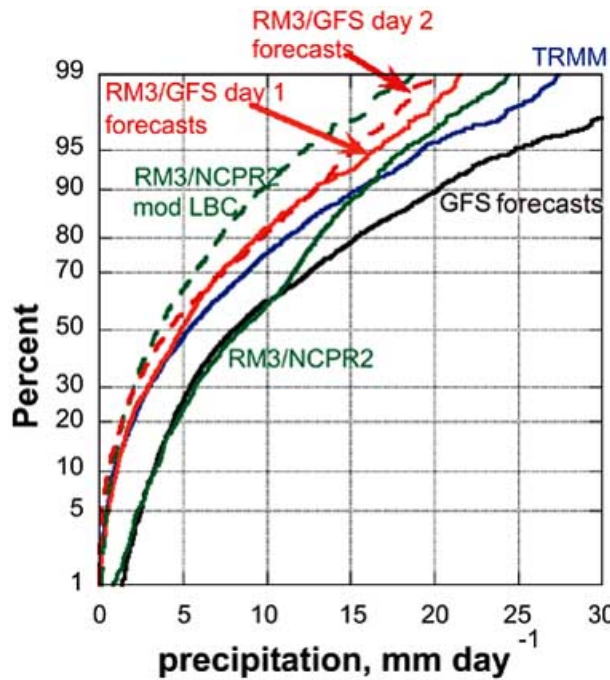


Fig. (4). Probability density distributions of each data set depicted in Fig. (3).

into a tropical depression on September 12th, into Tropical Storm Helene on September 14th and into Hurricane Helene on September 16th (see Brown [17]). The following figures show circulation and precipitation distributions of the incipient disturbance over West Africa on September 10, 2006. NCPR2 and RM3/NCPR2 circulations are quite similar at 700 mb (Fig. 5a, b) and 925 mb (Fig. 5c, d). A rather sharp 700 mb trough intersects 10°N, 5°W and a broad cyclonic circulation at 925 mb is centered over 13°N, 7°W, indicating an upward, southeasterly tilt. Both TRMM and RM3/NCPR2 produce a circular area of heavy precipitation (Fig. 5e, f) close to the 925 mb low center and downstream of the upper trough, as well as a band of precipitation along the Atlantic coast related to lower tropospheric onshore circulation. FEWS (Fig. 5g) shows a broader, more contiguous shield of precipitation over West Africa, but confirms the maximum near 13°N, 7°W and the clear area to the southeast. The 24 hour precipitation accumulations for September 10 from the continuous RM3 integration forced

by modified NCPR2 LBC, are shown in Fig. (5h). Comparison to Fig. (5f) shows that the modifications to the LBC eliminate much of the unrealistic light rain, but also decrease the maxima. Table 3 gives validation statistics for Area 1 for the simulated precipitation fields shown in Fig. (5f, h). The continuous simulation with modified NCPR2 forcing eliminates most of the bias of the unmodified control run, lowers the rms error and increases the spatial correlation with TRMM for September 10. Fig. (6) shows that this simulation reduces the lowest 90% of precipitation values producing a better match with TRMM, but it slightly underestimates the highest 10%. Table 3 also shows that the Area 1 validation statistics for the September 10 RM3/GFS FCST initialized at 00 UT on September 9 are slightly better than those for the forecast initialized 24 hours later.

Fig. (7a, b) show the 700 mb circulations for the 24-hour RM3/GFS FCST and GFS FCST, respectively. The RM3 nested version places the 700 mb trough in the same position as NCPR2 (Fig. 5a), but displaces the center of circulation several degrees to the south. The GFS GCST trough axis is about 2° longitude westward of the other versions at 10°N, but otherwise similarly located. RM3/GFS FCST (Fig. 7c) places the near surface low some 4° north of NCPR2 (Fig. 5c) and RM3/NCPR2 (Fig. 5d), while the driving model (Fig. 7d) produces a double center that envelops both locations.

The RM3/GFS FCST precipitation maximum (Fig. 7e) marks the position of the developing wave, although maximum rates are lower than TRMM. Nevertheless, this depiction is an improvement over the original GFS FCST (Fig. 7f), which predicts rates in excess of 300 mm during 24 hours. Fig. (6) shows that the highest 20% of September 10 GFS FCST precipitation encompasses values that are considerably greater than the highest 20% of TRMM or of the nested RM3 forecast. The highest TRMM accumulation for September 10th is 75 mm at 12.5°N, 8°W; for FEWS in this vicinity the maximum is about 50 mm and 41 mm are simulated by RM3/GFS FCST at 11°N, 7°W. The GFS FCST also predicts accumulations of more than 100 mm near 10°N, 6°E that are not substantiated by TRMM or FEWS. Both the original and the nested RM3/GFS FCST underestimate precipitation near the coast of Africa.

3.3. Real-Time Forecast: June 24, 2009

Fig. (8) shows an example of a real-time RM3 forecast made at ACMAD, driven by operational GFS data. Fig. (8a) shows RM3 24-hour precipitation accumulations for June 24, 2009, which should be compared to corresponding estimates of the actual rainfall from FEWS (Fig. 8b) and TRMM (Fig. 8c). Note that the TRMM shown is the experimental near real-time version, which usually changes in the more permanent archive. Both FEWS and TRMM show moderate rainfall along the Gulf coast, including maxima in excess of 55 mm. Both also show a maximum off the coast centered on 6°N, 17°W. The RM3 forecast also shows high accumulations along the southwest coast, and including the area around 6°N, 17°W, but it indicates too broad an area over the Gulf. Two areas of precipitation marked by the RM3 near 30°W also correspond to TRMM “observed” maxima. The more southerly area was adversely affected by proximity to the western computational boundary. Note that FEWS does not provide observations over the mid-Atlantic.

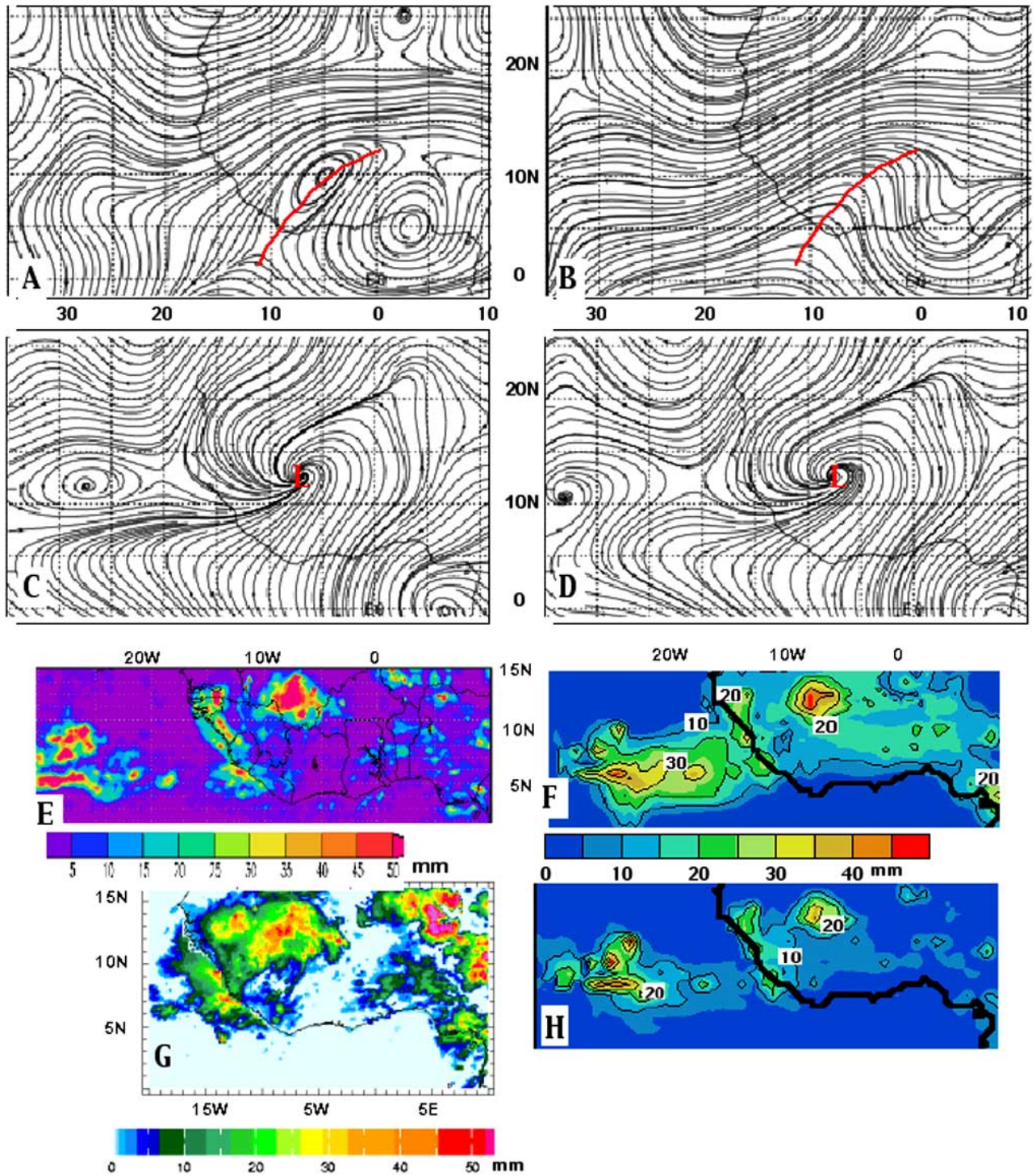


Fig. (5). Streamlines and precipitation accumulations for September 10, 2006: **a)** 700 mb streamlines (closer spacing of streamlines indicates higher wind speeds) based on NCPR2, **b)** as in (a), but for RM3/NCPR2, **c)** 925 mb streamlines based on NCPR2, **d)** as in (c), but for RM3/NCPR2, **e)** TRMM precipitation accumulations (mm), **f)** as in (e), but for RM3/NSPR2, **g)** as in (e), but for FEWS, **(h)** as in (e), but for RM3/NCPR2 with modified initial conditions at 00 UT on September 10, 2006 and modified LBC.

4. DISCUSSION AND CONCLUSIONS

This preliminary study evaluates GFS daily weather forecasts over West Africa and the adjacent Atlantic, made

by nesting a regional atmospheric model on a 0.5° grid. The regional model is the RM3 of GISS/CCSR. Daily first and second day forecasts were produced for September 1-30,

2006, the special observing period #3 of the African Monsoon Multidisciplinary Analysis. Simulated precipitation is compared here mostly to TRMM, but with reference also to FEWS. Since model simulations and TRMM estimates are derived from totally independent data, agreement is taken as a validation of both systems, although agreement could also imply that they share similar biases.

Table 3. Validation Statistics for Modeled Precipitation Accumulations within the Area 5-12°N, 20°W-10°E on September 10, 2006 Against Corresponding TRMM Estimates. Numbers in Parentheses Indicate the Bias and the rms Error as Percentages of the TRMM Area Mean Accumulation of 6.1 mm

	Bias	rms Error	Correlation Coefficient
RM3/NCPR2	+8.5 mm (139%)	11.7 mm (192%)	0.54
RM3/NCPR2 with modified LBC	+0.4 mm (7%)	5.7 mm (93%)	0.80
RM3/GFS FCST first day	+3.7 mm (62%)	9.0 mm (148%)	0.58
RM3/GFS FCST second day	+1.7 mm (28%)	8.3 mm (136%)	0.60
GFS FCST	+9.8 mm (161%)	27.6 mm (452%)	0.31

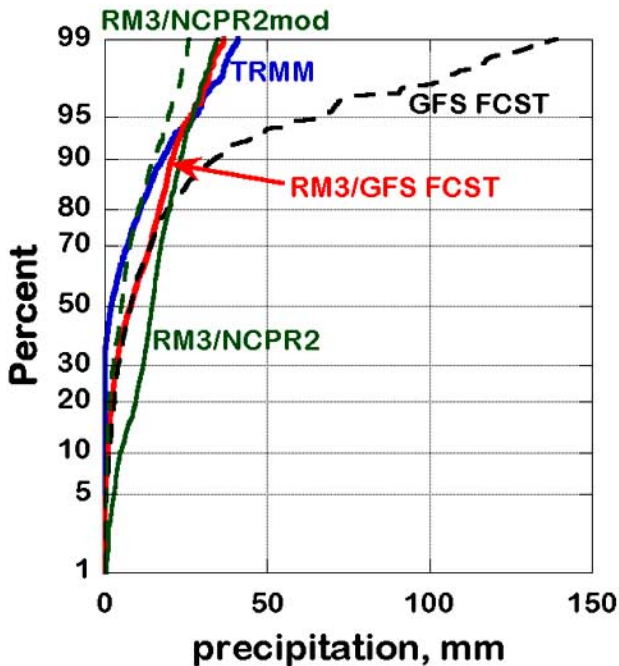


Fig. (6). Probability density distributions of precipitation accumulations on September 10 over Area 1: blue: TRMM, red: RM3/GFS FCST, black: GFS FCST, green solid: RM3/NCPR2 with modified LBC, green broken: RM3/NCPR2.

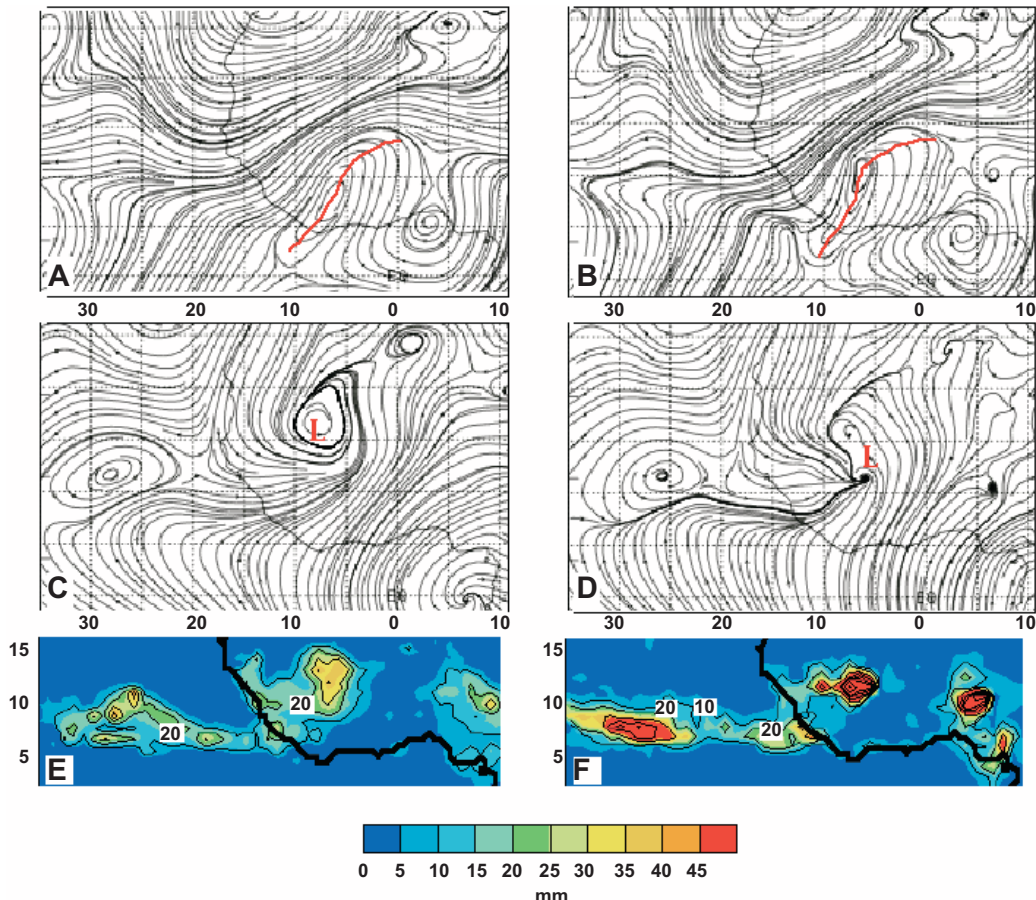


Fig. (7). Streamlines and precipitation accumulations for September 10, 2006: **a**) 700 mb streamlines (closer spacing of streamlines indicates higher wind speeds) based on RM3/GFS FCST, **b**) as in (a), but for GFS FCST, **c**) 925 mb streamlines based on RM3/GFS FCST, **d**) as in (c), but for GFS FCST, **e**) RM3/GFS FCST precipitation accumulations (mm), **f**) as in (e), but for GFS FCST.

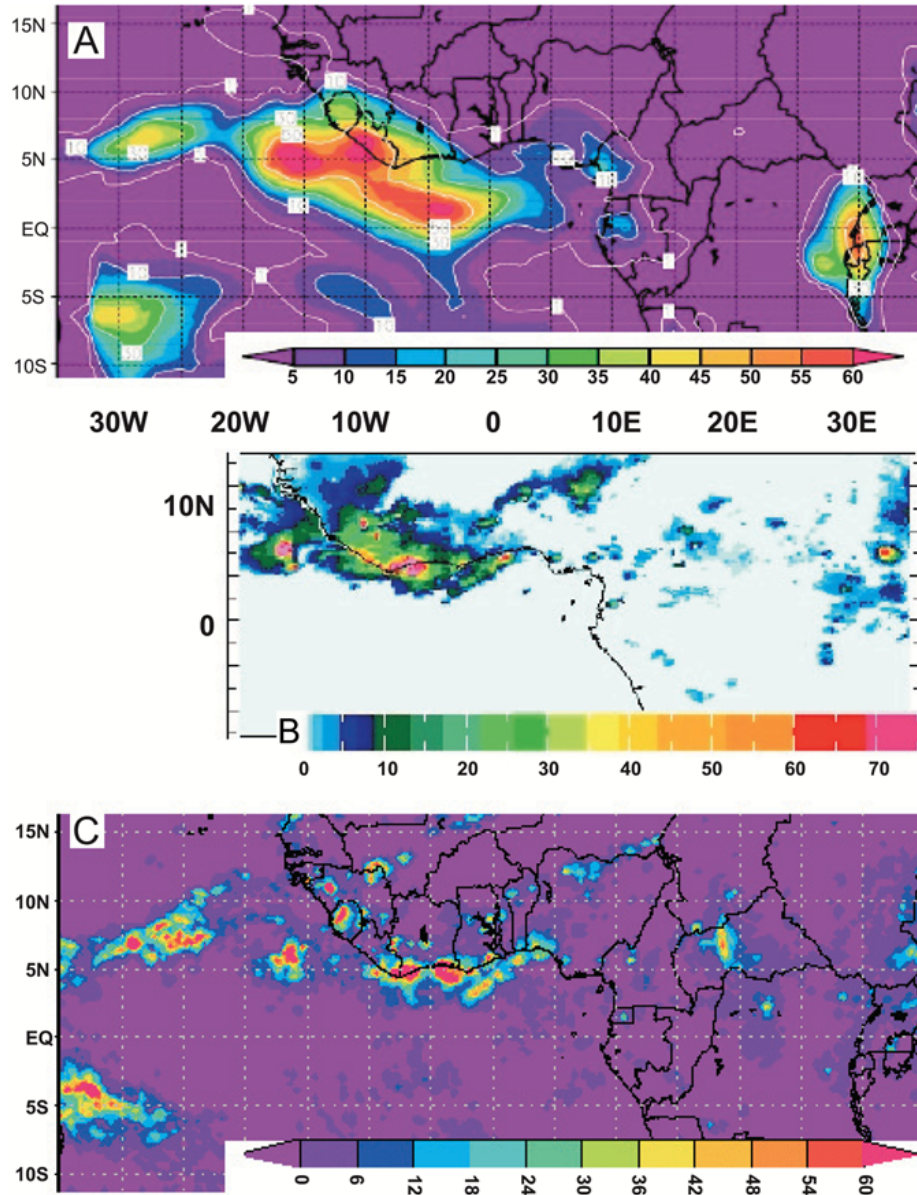


Fig. (8). Precipitation accumulations for June 24, 2009. **a)** RM3 real-time forecast made at ACMAD, forced by GFS data; **b)** FEWS, **c)** TRMM experimental near real-time estimates. Units: mm.

GFS global model 24-hour precipitation accumulations examined for September 2006 over the West African monsoon region are 65% rainier than corresponding TRMM estimates, which in turn are consistent with FEWS data. Untreated GFS initial and lateral boundary conditions drive nested RM3 forecasts that are unrealistically rainy. An empirical modification re-computes initial and boundary conditions such that forecast scores improve and the simulated low-level moisture advection toward the ITCZ and the West African rain belt is reduced by about 33%. The research confirmed the importance of spinning up the initial conditions with the regional model.

Experimental nested first day forecasts monitored in the rain belt for the 30 days of September have almost no bias compared to TRMM and a spatial correlation of 0.60, compared to only 0.32 for the GFS global product over the

same area. The correlation of the nested precipitation forecasts with TRMM within the area decreases to 0.55 for the second day. RM3 simulations forced with NCPR2 lateral boundary conditions improve the spatial correlation to 0.84. The time-longitude distribution of daily RM3 precipitation forecasts for September 2006 covering parts of West Africa and the adjacent Atlantic achieves a 0.77 correlation with corresponding TRMM archived data, a big improvement over the parallel correlation of only 0.37 for the GFS model. The nested RM3/GFS forecast captures the track of maximum precipitation associated with the pre-Helene storm that crossed the Atlantic coast on September 12 (Druyan *et al.* [7]).

In the single case study relating to an African wave disturbance on September 10, 2006, nesting on the 0.5° grid changed details of the GFS 700 mb and 925 mb streamline

patterns. The GFS parent model accurately located the storm's precipitation shield, but exaggerated 24 hour accumulations by as much as 400%. The RM3 created much more realistic accumulations along a trajectory confirmed by TRMM data.

Validation statistics need to be organized for a much larger sample of forecasts, representing other parts of the summer and multiple seasons. Testing will suggest additional refinements for optimization, which should take into account simulations of temperature, humidity and circulation as well as precipitation. Refinements will be shared with ACMAD for the continuation of operational numerical weather prediction.

ACKNOWLEDGEMENTS

This research was supported by National Science Foundation grant ATM-0652518, National Aeronautics and Space Administration (NAMMA) grant NNX07A193G and by the National Aeronautics and Space Administration Climate and Earth Observing System Program. TRMM images and data used in this study were acquired using the GES-DISC Interactive Online Visualization ANd aNalysis Infrastructure (Giovanni) as part of the NASA's Goddard Earth Sciences (GES) Data and Information Services Center (DISC). FEWS data are compiled by the NOAA Climate Prediction Center and are archived by the International Research Institute for Climate and Society, Columbia University.

REFERENCES

- [1] Redelsperger JL, Thorncroft CD, Diedhiou A, Lebel T, Parker DJ, Polcher J. African monsoon multidisciplinary analysis: an international research project and field campaign. *Bull Am Meteorol Soc* 2006; 87: 1739-46.
- [2] Nuret M, Lafore J-P, Asencio H, et al. Evaluation of METEO-FRANCE numerical weather prediction models during AMMA 2006-SOP. *Aladin Newslett* Nr. 32, 2007; 32: 93-107.
- [3] Druyan L, Feng J, Cook K, et al. The WAMME regional model intercomparison study. *Clim Dynam* 2009; doi 10.1007/s00382-009-0676-7.
- [4] Reed R, Klinker E, Hollingsworth A. The structure and characteristics of African easterly wave disturbances as determined from the ECMWF operational analysis/forecast system. *Meteorol Atmos Phys* 1988; 38: 22-33.
- [5] Druyan L, Fulakeza M, Lonergan P. Mesoscale analyses of West African summer climate: focus on wave disturbances. *Clim Dyn* 2006; 27: 459-81.
- [6] Druyan L, Fulakeza M, Lonergan P. The impact of vertical resolution on regional model simulation of the west African summer monsoon. *Int J Climatol* 2008; 28: 1293-1314.
- [7] Druyan L, Fulakeza M, Lonergan P, Noble E. Regional climate model simulation of the AMMA special observing period #3 and the pre-helene easterly wave. *Meteorol Atmos Phys* 2009; 103: 191-210.
- [8] Xue Y, Lau K-M, Cook K, et al. The West African monsoon modeling and evaluation project (WAMME) and its first model intercomparison experiment. *Bull Am Meteorol Soc* 2009; (Submitted).
- [9] Campana K, Caplan P, Alpert J, et al. Technical Procedures Bulletin for the T382 Global Forecast System. 2005. Available from: http://www.emc.ncep.noaa.gov/gc_wmb/Documentation/TPBoct05/T382.TPB.FINAL.htm
- [10] Global Climate and Weather Modeling Branch. The GFS Atmospheric Model. NCEP Office Note 442, Environmental Modeling Center, Camp Springs MD, 2003. Available from: <http://www.emc.ncep.noaa.gov/officenotes/newernotes/>
- [11] Kanamitsu M, Ebisuzaki W, Woollen J, et al. NCEP-DOE AMIP-II reanalysis (R-2). *Bull Am Meteorol Soc* 2002; 83: 1631-43.
- [12] Huffman GJ, Adler RF, Arkin P, et al. The global precipitation climatology project (GPCP) combined precipitation dataset. *Bull Am Meteorol Soc* 1997; 78: 5-20.
- [13] Ruane A, Roads J. 6-Hour to 1-year variance of five global precipitation sets. *Earth Interact* 2007; 11: 1-29.
- [14] Herman A, Kumar V, Arkin P, Kousky J. Objectively determined 10-day African rainfall estimates created for famine early warning systems. *Int J Remote Sens* 1997; 18: 2147-59.
- [15] Druyan L, Fulakeza M. Mesoscale climate analysis over West Africa. *CLIVAR Exchanges* 2005; 34 (3): 20: 34-5.
- [16] Schmidlin FJ, Morrison BJ, Northam ET, Gerlach J. Detailed observations of five African Easterly waves during NAMMA. In: Proceeding of a workshop, NAMMA Science Team Meeting, Baltimore MD, May 2007.
- [17] Brown D. Tropical Cyclone Report, Hurricane Helene (AL082006), National Hurricane Center, NOAA: Miami FL 2006.

Received: July 7, 2009

Revised: September 4, 2009

Accepted: September 10, 2009

© Druyan et al.; Licensee Bentham Open.

This is an open access article licensed under the terms of the Creative Commons Attribution Non-Commercial License (<http://creativecommons.org/licenses/by-nc/3.0/>) which permits unrestricted, non-commercial use, distribution and reproduction in any medium, provided the work is properly cited.